

Multi-objective optimization of low moisture food extrusion processing through active learning and robotics

Deborah Becker ^{*a,b}, Jean-Vincent Le Bé ^a, Cornelia Rauh ^b, Christoph Hartmann ^{c,b}

^a Nestlé Institute of Food Sciences, Nestlé Research, Lausanne 1000, 26, Switzerland

^b Institute of Food Technology and Food Chemistry, Technische Universität Berlin, Berlin 14195, Germany

^c Strategic Research Operations, Nestlé Research, Lausanne 1000, 26, Switzerland

ARTICLE INFO

Keywords:

Extrusion
Multi-objective Bayesian optimization
Machine learning
Expanded snacks
Automated analytical platform

ABSTRACT

As low-moisture extrusion processing is very complex, especially due to the high number of process variables and their strong interdependence, experimental approaches in product development typically involve numerous iterations accompanied by off-line product testing. These processes are resource-intensive, time-consuming, and require expert knowledge. To overcome these limitations, this study presents a closed-loop framework that links automated product characterization with multi-objective optimization to configure the extruder's operating variables for achieving specific product characteristics. For this purpose, an on-line automated analytical system based on gravimetric and visual techniques was developed, with results directly fed into the Thompson Sampling Efficient Multi-Objective Optimization (TSEMO) algorithm. The process parameters to be optimized were the barrel zone temperatures, screw and cutter speed, total feed moisture and the feed rate. Objectives for the total throughput, bulk density, shape and expansion ratio of the extrudates were pre-defined. The results of this study demonstrate an efficient approximation of those target properties within 15 iterations, while identifying optimal extrusion settings in a high-dimensional process space. This approach highlights the potential of integrating automation and active learning algorithms for the optimization of low moisture extrusion processes and offers a promising tool to accelerate the process development of directly expanded food products.

1. Introduction

Extrusion is a multi-purpose technology characterized by high shear, high temperature, high pressure and short processing times. While this process is commonly described in shorthand as a procedure in which food ingredients are forced through a die, it combines multiple operations, including conveying, kneading, heating, mixing and shaping (Riaz, 2019). Furthermore, it enhances the product texture by modifying starch and protein structures and improves digestibility by breaking down complex molecules. A safe food product is ensured due to the high temperature processing, which eliminates harmful microbes (Egal and Oldewage-Theron, 2019; Morantes et al., 2020). As a result, this technology plays an important role in food manufacturing and is widely used in the production of meat analogs, cereals, snacks, and pet food.

The latter three fall into the category of direct-expanded products, which are processed under low moisture conditions of the feed, typically below 30 % (wet basis) (Lai and Kokini, 1991; Bouvier and Campanella, 2014) and a melt temperature at the die ranging from 100 to 160 °C

(Chinnaswamy and Hanna, 1988). The main ingredients in these products are usually cereal grain flours with high starch content. Due to the low moisture content, the mechanical energy input is high and generates strong shear forces, which lead to considerable molecular degradation of the starch. This results in the formation of a porous structure and therefore the characteristic light and crispy texture of direct-expanded products (Ek and Ganjyal, 2020). Although these starch-rich extrudates are energy-dense, they often lack a variety of essential nutrients. In recent years, the demand for nutrient-rich foods has increased significantly, which is why the use of alternative ingredients, or their fiber- and protein-rich components has gained in importance. Latest research has therefore focused on enhancing the nutritional properties of direct-expanded products without compromising their overall quality (Gomes et al., 2023; Shah et al., 2022; Patil and Kaur, 2018).

In order to achieve the required product characteristics, it is essential to adapt the extrusion conditions, such as temperature, screw speed, moisture content, according to the composition, structure and natural variability of alternative raw materials. Due to the multivariate nature

* Corresponding author at: Nestlé Institute of Food Sciences, Nestlé Research, Lausanne 1000, 26, Switzerland.

E-mail address: deborah.becker@rd.nestle.com (D. Becker).

and the complex cause-effect relationships of the extrusion process, recipe adaptation or new product development results in high experimental effort.

To master this challenge, mathematical modelling approaches have become increasingly important tools in process optimization. These models reduce the need for extensive trial-and-error experimentation, thereby minimizing waste and downtime. In addition, they enable a deeper understanding of the underlying mechanisms during extrusion. This is especially relevant given the high cost of food extrusion equipment, which makes it impractical to customize hardware for each individual operation. Instead, adapting process parameters for each specific formulation or product goal represents a more flexible and cost-effective strategy. A good example of this approach can be found in plastics and polymer technology, where mathematical modeling and numerical simulations are now standard procedures (Kristiawan et al., 2020). These advances have since been adapted to food extrusion. Here, the more complex and variable properties of the raw materials lead to a greater challenge in accurate modeling, but the latter also represents a great opportunity.

Response Surface Methodology is probably the most popular approach for optimizing extrusion conditions, primarily due to its simplicity. However, its main drawbacks include the exponential increase in the number of experiments required as the number of parameters studied grows and the limited validity of results outside the experimental domain (Tachibana et al., 2023). As a result, machine learning techniques such as Artificial Neural Networks have become more common (Fan et al., 2013; Mitra and Ramaswamy, 2021), along with the use of Genetic Algorithms and hybrid approaches that combine these three methods (Kojic et al., 2019; Kowalski et al., 2018, 2021).

More recently, probabilistic and data-efficient methods such as Bayesian Optimization (BO) have gained attention, due to their ability to optimize in real-time and iteratively with only limited data. BO uses machine learning techniques to strategically guide experimentation with fewer trials while increasing the likelihood of identifying optimal processing conditions. By building a probabilistic surrogate model, such as Gaussian Processes, followed by an acquisition function, BO balances exploitation (refining known promising regions of the input parameter space) and exploration (investigating under-sampled regions with high uncertainty). This dynamic search mechanism allows BO to focus on the most promising combinations of input parameters that are expected to give the greatest improvement. The successful application of BO in a variety of non-food domains (Fulkerson et al., 2024; Myung et al., 2025), as well as in food formulation (Becker et al., 2023) and high-moisture extrusion (Theng et al., 2025) highlights its strong potential to enhance process optimization in low-moisture extrusion.

In addition, the optimization of the extrusion conditions is often challenged by the limitations of conventional product characterization methods. Most analytical techniques used to evaluate extrudate properties, e.g. water absorption index (WAI) and water solubility index (WSI), texture analysis, bulk density and more, rely on off-line or at-line measurements, which introduce delays in both product assessment and process adjustments. This time lag makes it challenging to achieve real-time process control.

Therefore, this study explores the use of a multi-objective Bayesian optimization framework, an algorithm called TSEMO, to enhance low moisture extrusion processes to produce direct expanded snacks. The framework models the relationships between critical extrusion process parameters, such as moisture content, feed rate, barrel temperature, screw speed, and cutter speed, and the desired product parameters, including expansion ratio, shape, bulk density and total throughput. The product parameters are assessed on-line and near real-time by a newly developed automated analytical platform that is integrated into the extrusion line. This iterative process combining experimentation, automated characterization and multi-objective optimization is expected to reduce the number of experiments required while maximizing the probability of achieving the desired product quality. This can potentially

overcome the limitations of current optimization methods and accelerate the development of direct- expanded extrusion products.

2. Materials and methods

2.1. Raw materials

Corn semolina (Refined semolina S50, Kalizea, 80–90 % starch) and defatted, toasted soybean flour (SOPRO-TB 200 A, SOJAPROTEIN, 51 % protein dry base) were used as dry ingredients during the extrusion trials. They were mixed in a ratio of 65 % corn semolina and 35 % soy flour. The moisture content of the mixture was determined with a rapid moisture analyzer and ranged between 9 – 10 %.

2.2. Extrusion process

Extrusion was performed using a 20 mm diameter co-rotating twin-screw extruder with a length-to-diameter (L/D) ratio of 20:1 (Model TwinLab B-TSE-S 20/40, Anton Paar, Graz, Austria). The extruder had four independently temperature-controlled zones and two heating rings at the die outlet, which together were defined as a fifth heating zone. A 3 mm cylindrical die was used for all trials. The screw configuration was specifically designed for the production of directly expanded products. Water flow was adjusted according to the feed rate and the initial moisture content of the mixture in order to achieve the desired total moisture content. Sensors for die pressure and temperature were installed at the extruder outlet. All relevant process data, including die temperature, die pressure, zone temperatures, motor torque, and specific mechanical energy, were automatically recorded at one-second intervals. To define the final product length, a rotating knife with six blades was installed at the extruder outlet. The soy–corn blend was delivered to the extruder via a gravimetric feeder. At the beginning of each trial, the extruder was initialized using a standardized start-up protocol. In this procedure, the process parameters were adjusted step by step until they reached predefined operating conditions that resulted in a reference product. This reference product was used as a comparison for evaluating the performance of the extruder in different trials, especially if these were carried out on different days.

2.3. Characterization of extrudates

To enable near real-time characterization of the product an automated analytical platform was developed and attached to the extrusion line. As shown in Fig. 1, the platform consists of two interconnected modules: one for sampling and gravimetric analysis and the other for image-based analysis.

The communication with all actuators and sensors, as well as the operation and coordination of both analytical modules, was controlled via a Python script. The entire automated process, from sampling to data acquisition, was completed in approximately three minutes per sample.

2.3.1. Module 1 – sampling and gravimetric analysis

This module is designed for automated sampling and the determination of bulk density and throughput. In Fig. 1 (left side) this part is indicated by a dark gray background and a magnified view (right side) shows the most important elements in detail. A transparent and cylindrical container (highlighted in blue in Fig. 1) with a 1-liter capacity and an open top is mounted on a linear rail system driven by a stepper motor. This setup allows the container to move precisely back and forth beneath the extruder outlet. Fixed limit switches ensure accurate positioning. To monitor the filling level, an LED is mounted above the container, with an ambient light sensor positioned directly opposite (highlighted in red in Fig. 1). As soon as the container is filled with extrudates, less light from the LED reaches the sensor and the sampling is stopped. A sliding lid is installed at the bottom of the container, which opens mechanically when the container reaches a specific position on the rail. The container itself

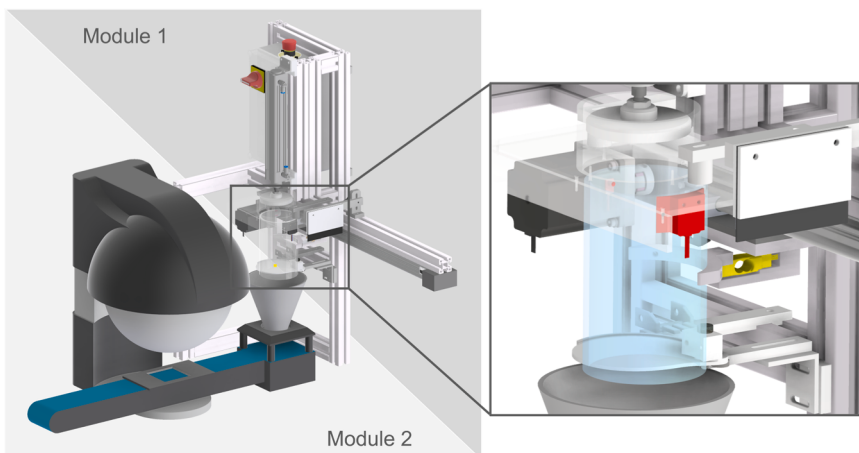


Fig. 1. Left side: 3D visualization of the automated analytical system for on-line product characterization of expanded extrudates. Right side: close-up of cylindrical container (blue) with load cell in yellow and ambient light sensor and LED in red.

is mounted on a load cell (highlighted in yellow in Fig. 1), so that the weight of the collected extrudates can be recorded in real-time. The automated analysis began when the extrusion process reached a stable state. The system first recorded the empty weight of the container, which then moved into a position directly beneath the extruder outlet, activating a timer. A funnel guided the extrudate from the outlet into the container to prevent material loss. When the light sensor signalized that the container was full, the timer stopped. The container then moved away from the outlet, and the fill weight was recorded. Using the measured weight and the elapsed time, the throughput was calculated. To determine bulk density, defined as the mass per unit volume, the container was moved back under the extruder and continued filling beyond the sensor threshold until it slightly overflowed. As it moved away from the outlet again, a fixed spatula removed any excess material, ensuring the container was filled exactly to the top edge. The bulk density then was calculated from the mass accumulated in the container of 1-liter un-tapped apparent volume. Finally, the container reached a predefined unloading position, where the mechanical sliding lid opened, allowing the product to fall into a funnel located below and thus be transferred to module 2. A vertically moving piston ensured complete emptying in case the extrudates adhered to the cylinder wall.

2.3.2. Module 2 – image analysis

The expansion ratio and the compactness were detected using the instrument and corresponding Software VideometerLab (VIDEOMETER, Herlev, Denmark). This device combines spectral imaging technology with machine learning for versatile and fast product characterization. For optimal and uniform illumination, 19 flash diodes (LEDs) with specific wavelengths between 365 nm (UV) and 970 nm (NIR) are placed in the center of a sphere (Carstensen and Følmer-Hansen, 2000). A high-resolution camera is installed on top of the sphere, whereas the sample is placed on the opposite side under an opening port.

Prior to any analysis, the system was calibrated using plates with solid white, solid black, and white dotted lines. Subsequently, the lightning configuration was adjusted to optimize illumination for the sample measurement, using a reference product placed on a blue plate. Blue was selected as the background color because it contrasts well with the yellow-toned samples. The choice of plate color was important for successful foreground/background discrimination, which was realized by nCDA (normalized Canonical Discriminant Analysis). This linear transformation provides a clear differentiation between the sample and the background (Carstensen, 2018). An operation of segmentation was applied to refine and divide the transformed digital image into discrete groups of pixels, where the desired objects (extrudates) are called blobs. In this specific case, small pixel clusters caused by dust on the

background surface, were removed and touching objects separated, so that the morphological information for each blob could be further extracted. The morphological features selected for this study were the projected cross-sectional area and the compactness (C_r , circular and length based). By dividing the cross-sectional area of the extrudates by the cross-sectional area of the extrusion die opening, the expansion ratio was calculated.

Compactness quantifies the degree to which the shape of an object approaches that of an ideal circle. This value was calculated as follows:

$$C_r(\%) = \frac{4 * A}{\pi * L^2} * 100 \quad (1)$$

L is hereby defined as the characteristic length of the blob, i.e. measuring how long an object is along its longest direction and A is the projected surface area. To enable automated image analysis of the product, the Videometer was connected to the corresponding VideometerLab Autofeeder system (VIDEOMETER, Herlev, Denmark). This Autofeeder comes with a vibration mechanism that distributed the extrudates from the funnel evenly onto a blue colored conveyor belt (see chapter 2.3.1). Via this belt the extrudates were transported under the opening of the sphere and in each measurement cycle a batch of 100 extrudates was analyzed.

2.4. TSEMO algorithm

The analytical platform and the optimization framework were in constant interaction. The optimization framework was based on the Thompson Sampling Efficient Multi-Objective Optimization (TSEMO) algorithm, as introduced by Bradford, Schweidtmann, and Lapkin (2018). TSEMO is designed to solve expensive black-box optimization problems by modeling each objective function using separate Gaussian processes, which serve as surrogate models. For a general overview of Gaussian processes, refer to Schulz, Speekenbrink, and Krause (2018). An initial dataset of 12 experiments was generated during a first trial (trial #1) using Latin Hypercube Sampling to efficiently cover the parameter space and create Gaussian process models, balancing data diversity with minimal experimental effort. During the optimization process (trial #2), the Gaussian processes were iteratively updated. For each iteration, Thompson Sampling was used to draw sample functions from the individual Gaussian processes. These samples were generated using spectral sampling, which enabled efficient function sampling in a high-dimensional space. For each sampled function, an approximate Pareto set was then identified using the NSGA-II algorithm (Deb et al., 2002), a fast and elitist multi-objective genetic algorithm. NSGA-II performs non-dominated sorting and uses crowding distance sorting to obtain a Pareto front. The resulting Pareto front provided a set of

potential sampling points for the next evaluation. To select the most promising one, the algorithm calculated the hypervolume improvement for each candidate point, i.e., the increase in the objective space dominated by the Pareto front if the point were added. The point with the highest hypervolume gain was selected for the next experiment, ensuring both exploration and exploitation were balanced effectively.

2.5. Closed-loop optimization procedure

The process was modeled as a multiple-input, multiple-output system, and a general schematic of the workflow is shown in Fig. 2. The input consisted of independent process parameters, which were set manually on the extruder by the operator. The parameters investigated included feed rate, total moisture content, screw speed, cutter speed, and the temperatures of the five barrel zones. The range for each variable, as outlined in Table 1, was determined based on literature data and in addition, nine data points covering the extreme values of screw speed, feed rate and moisture content were tested experimentally. These operating conditions were selected to ensure stable material flow while avoiding excessive pressure and torque that could disrupt the extrusion process.

Since the optimization loop ran in real-time without pausing the extrusion, parameters related to the geometry of the extruder and formulation were kept constant throughout the trials. Under these controlled settings, the extruded product exhibited specific physical characteristics. In this study, four product parameters were monitored: bulk density (ρ_d), total throughput (\dot{m}_{out}), expansion ratio (ER), and compactness (C_r). Those parameters represent a trade-off between process efficiency (productivity and cost-efficiency through high throughput) and product quality, especially structural product properties. Furthermore, it is possible to analyze these parameters in near real time and in-line without human input and the interruption of the extrusion process. The optimization objectives (Eq. (2)) were defined as maximizing throughput, compactness, and expansion ratio, while minimizing the deviation in bulk density compared to a reference sample, hence

$$\text{minimize}[\Delta\rho_d, -\dot{m}_{out}, -ER, -C_r]. \quad (2)$$

The bulk density of the reference sample was 160 g/L, a value that was achieved during the preliminary tests and can also be found in the literature for comparable formulations (Sahu et al., 2022). At each iteration, the operational conditions of the extruder were adjusted based on the process parameters recommended by the optimization algorithm. Once the extrusion process reached a stable state, the resulting product

Table 1
Upper and lower bound of independent process parameters.

Process variable	Lower bound	Upper bound
Feed rate [kg/h]	9.5	15.5
Total moisture [%]	16	20
Screw speed [rpm]	300	500
Temperature zone 1 [°C]	30	70
Temperature zone 2 [°C]	30	100
Temperature zone 3–5 [°C]	100	140
Cutter speed [rpm]	300	500

was analyzed by the robotic system. The corresponding process and product data, including the measured temperature values from each barrel zone, were then fed into the TSEMO algorithm. Based on all previous experiments, the algorithm proposed a new set of process parameters for the next iteration. This procedure was repeated until the predefined stopping criterion was met, which was set at a maximum of 15 iterations.

3. Results and discussion

The 12 sample points of the initial data set were processed through the extruder during trial #1 in a randomized order and analyzed using the robotic system. As expected, variations in extrusion parameters influenced the characteristics of the direct-expanded corn-soy products. In addition, no excessive pressure or torque values were observed throughout this trial, and all parameter configurations resulted in analyzable products. The expansion ratio ranged from 1.62 to 2.74, the circularity from 37 – 92.5 %, while the difference in bulk density spanned from 53.2 to 360 g/L and the total throughput from 9.24 to 13.58 kg/h. The specific process parameters, including actual measured temperatures, and the corresponding product properties are summarized in Table 2.

The complete set of process and product parameters from trial #1, including measured temperature values, were used as input for the TSEMO algorithm and to initiate the optimization process. The loop of extrusion, robotic analysis, and optimization was then repeated 15 times. The outcomes are visualized in Figs. 3, 4 and 6, each showing the 12 initial data points along with the 15 additional samples generated through the optimization process. The blue triangles represent the initial data set from trial #1, while the red circles are sample points from the optimization process in trial #2. Filled markers indicate Pareto-optimal samples, which are those that offer the best trade-offs between the different objectives without one being improved at the expense of

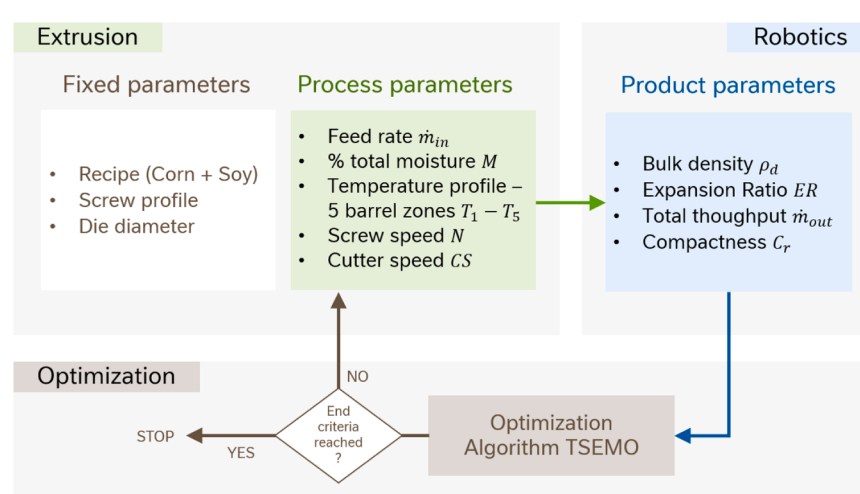


Fig. 2. Workflow representing the closed loop of the three elements: extrusion, automated analysis via robotics and optimization, as well as the input (process) and output (product) parameters.

Table 2

Process and product parameters from trial #1 and trial #2.

	Sample	Process parameter												Product parameter					
		Screw speed (rpm)	Cutter speed (rpm)	Feed rate (kg/h)	Total moisture (%)	$T_{1,t}$ (°C)	$T_{1,m}$ (°C)	$T_{2,t}$ (°C)	$T_{2,m}$ (°C)	$T_{3,t}$ (°C)	$T_{3,m}$ (°C)	$T_{4,t}$ (°C)	$T_{4,m}$ (°C)	$T_{5,t}$ (°C)	$T_{5,m}$ (°C)	$\Delta\rho d$ (g/L)	\dot{m}_{out} (kg/h)	ER (-)	C_r (%)
Initial data set – trial #1	1	360	400	10.7	17.7	41	38	84	82	121	122	120	119	136	136	53.2	9.97	2.53	90.9
	2	400	470	12	18.8	43	43	89	88	136	135	104	121	122	124	58.1	11.35	2.56	92.5
	3	440	440	9.6	20	37	35	96	97	105	105	109	110	100	100	223.2	9.24	2.05	88.3
	4	380	340	14.4	19.5	60	60	99	99	122	122	104	100	106	107	360.0	13.58	1.69	37.0
	5	350	490	12.2	19.3	44	39	66	84	137	137	133	133	132	132	36.5	11.25	2.64	92.2
	6	330	350	11.1	19.1	46	44	62	61	109	111	112	114	119	119	361.8	10.39	1.66	51.2
	7	450	310	10.1	19.7	50	51	42	70	112	112	128	128	130	130	62.0	9.43	2.74	84.9
	8	320	380	11.4	18.4	32	30	38	49	115	115	123	123	110	110	344.6	11.27	1.62	53.1
	9	420	320	13.8	18.1	63	62	72	75	130	130	125	125	135	135	316.4	10.77	1.79	49.6
	10	470	310	10.2	18.6	66	66	76	76	102	102	118	118	103	103	258.7	9.52	1.99	64.8
	11	410	410	12.8	17.2	51	51	48	48	101	101	134	134	116	116	303.4	11.87	1.74	55.1
Optimization data set – trial #2	12	490	370	13.1	16.5	55	55	45	45	127	127	116	116	112	112	252.8	12.22	1.94	87.1
	1	360	390	10.2	19.6	39	40	90	88	106	109	124	124	102	102	183.4	156	2.2	87.06
	2	340	410	12.4	18.7	57	58	43	73	135	137	100	114	127	127	109.9	192	2.48	84.3
	3	370	420	10.3	19	37	34	90	88	122	122	107	113	130	130	158.0	160	2.24	88.35
	4	360	420	9.8	18.5	47	47	92	93	123	123	132	135	123	125	35.0	150	2.67	91.84
	5	320	500	10.7	18.8	47	47	78	80	139	137	123	124	124	124	100.0	165	2.33	91.89
	6	330	470	10.3	18.3	48	48	84	83	135	135	103	132	132	131	35.0	156	2.59	92.14
	7	410	470	11	18	52	53	83	83	137	137	106	131	140	141	28.0	163	2.92	91.1
	8	460	490	12.1	16.9	59	59	77	86	140	140	105	138	129	129	56.0	180	3.33	91.6
	9	370	440	12.6	17.2	41	41	65	82	140	139	102	142	107	108	57.0	185	3.4	91.8
	10	430	430	9.5	16.5	30	31	61	75	140	140	120	127	140	140	67.0	144	3.23	92.16
	11	450	400	9.7	16.5	30	31	80	80	136	135	103	125	136	136	60.0	147.4	3.27	92.13
	12	470	500	11.3	17	50	50	31	63	140	140	100	111	130	130	58.0	170.1	3.19	92.2
	13	400	300	9.5	16.2	58	58	69	84	134	134	111	133	111	110	68.7	140	3.57	82.2
	14	420	350	11.4	17.8	44	40	98	98	140	140	100	128	127	127	54.8	171.8	3.67	88
	15	460	420	12	17.3	46	46	96	96	140	140	125	128	120	121	68.2	180.2	3.51	89.8

$T_{1,t} - T_{5,t}$: target temperatures suggested by TSEMO for zones 1–5, $T_{1,m} - T_{5,m}$: measured temperatures, $\Delta\rho d$: absolute value of the deviation in bulk density to reference sample, \dot{m}_{out} : total throughput, ER: expansion ratio, C_r : compactness.

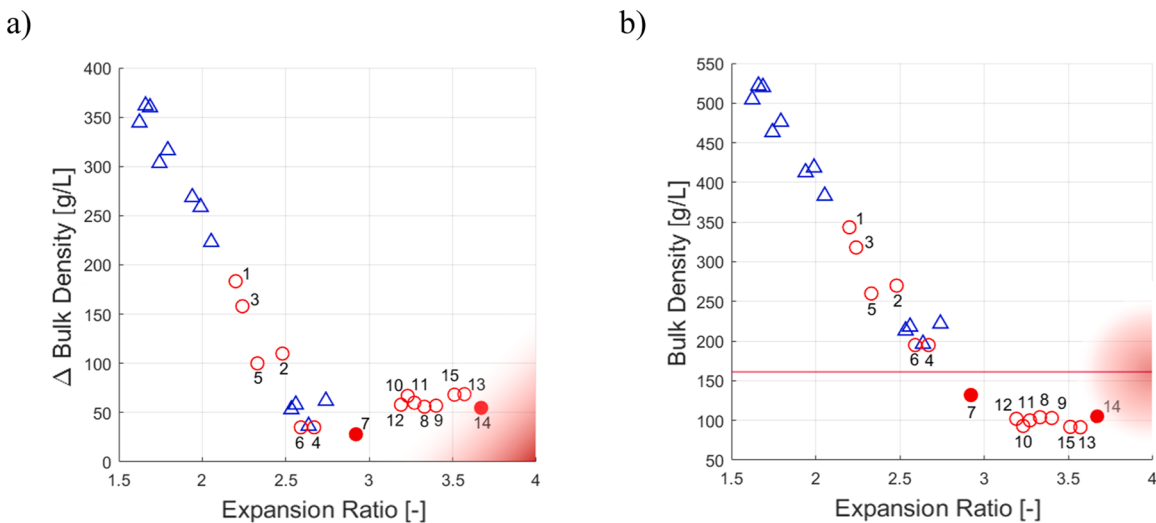


Fig. 3. Results and pareto front (●) between the expansion ratio and the a) difference in bulk density, as well b) absolute bulk density from trial #1 △ and #2 ○. The optimal region of the design space defined by the objectives is indicated by the red shaded area.

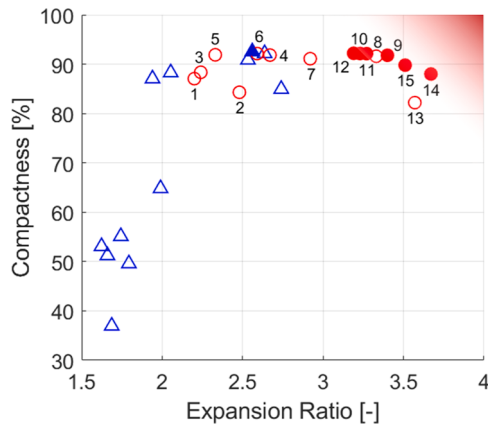


Fig. 4. Results and pareto front (●, △) between the expansion ratio and the compactness from trial #1 △ and #2 ○. The optimal region of the design space defined by the objectives is indicated by the red shaded area.

another. The red-highlighted zone in the plot marks the optimal region based on the specified target criteria.

In Fig. 3a), which presents the relationship between the bulk density differences and expansion ratio, a clear negative correlation is observed until an expansion ratio of 3. As the expansion ratio increases, the change in bulk density decreases.

This trend meets theoretical expectations, as expansion occurs when the water rapidly evaporates under ambient conditions as it leaves the high-pressure extruder and air cells form within the product matrix. Higher expansion typically reflects greater air incorporation, resulting in a lighter, more voluminous structure and consequently a lower bulk density (Morales Alvarez, 2020). This section of negative correlation contains all the sample points from the initial data set as well as the samples from the first seven iterations of the algorithm. All the other samples proposed by TSEMO (O8-O15) are concentrated in a region of greater expansion but only minor changes in density difference. This behavior can be observed even more precisely in Fig. 3b) where the absolute value of bulk density is plotted against the expansion ratio. The target value of 160 g/L of the reference product is marked with a red horizontal line. As in Fig. 3a), a plateau in bulk density data is recognizable, with values of the absolute bulk density clustering around 100 g/L. This indicates that the observed differences in bulk density

primarily result from samples, with a density below the desired target. Process parameters which, according to the literature, have an influence on extrudate expansion are moisture content, barrel temperature and screw speed. Several studies have shown that an increase in moisture content typically leads to lower expansion, while a higher screw speed and barrel temperature tend to increase expansion (Mezreb et al., 2003; Ditudompo et al., 2016; Kaur et al., 2022). The opposite effect of these process parameters was observed for the bulk density of soy enriched corn extrudates, where higher screw speed and temperature, and lower moisture, lead to decreased bulk density (Sahu et al., 2022). The progression of temperature (zone 3), screw speed, and total moisture values in the optimization data points in Table 2 indicates that TSEMO was able to identify the underlying correlations between those process parameters and expansion/ bulk density based on the initial 12 data points and continued to reinforce this pattern throughout subsequent iterations. Beyond this, it was possible to further increase the expansion through suitable adaptation of the input parameters without lowering the bulk density. The Pareto-optimal samples detected in Fig. 3a) and b) are the data points O14 and O7, demonstrating a favorable combination of high expansion and smallest achievable bulk density difference.

Fig. 4 shows the relationship between the compactness and expansion ratio. During the initial data set an overall increasing trend is observed, with values for compactness rising alongside the expansion ratio. This is particularly noticeable in the range of low expansion ≤ 2 .

For extrudates with low expansion, the ratio of throughput to cutter speed has a major impact on the final shape. With the resulting throughputs and the fixed upper limit of the cutter speed, the length of the products is greater than the cross-sectional diameter, resulting in elliptically shaped extrudates. The optimization algorithm immediately focuses on the region of high compactness, as seen by the clustering of the first sample points from trial #2 near the top of the plot. From this starting position, the algorithm progressively improves the expansion ratio while maintaining consistently high compactness values. This trend is clearly reflected in the images of the samples shown in Fig. 5.

Early samples already exhibit relatively high roundness, while subsequent Pareto-optimal samples such as O9, O10, O11, O12, O14 and O15 display not only high roundness but also progressively more expanded shapes. TSEMO can therefore successfully map the function between the process parameters and the roundness based on the 12 data points.

In Fig. 6, the total throughput is plotted against the expansion ratio. The initial data set spans a broad range of values. Unlike the previous figures for bulk density and compactness, the optimization samples in

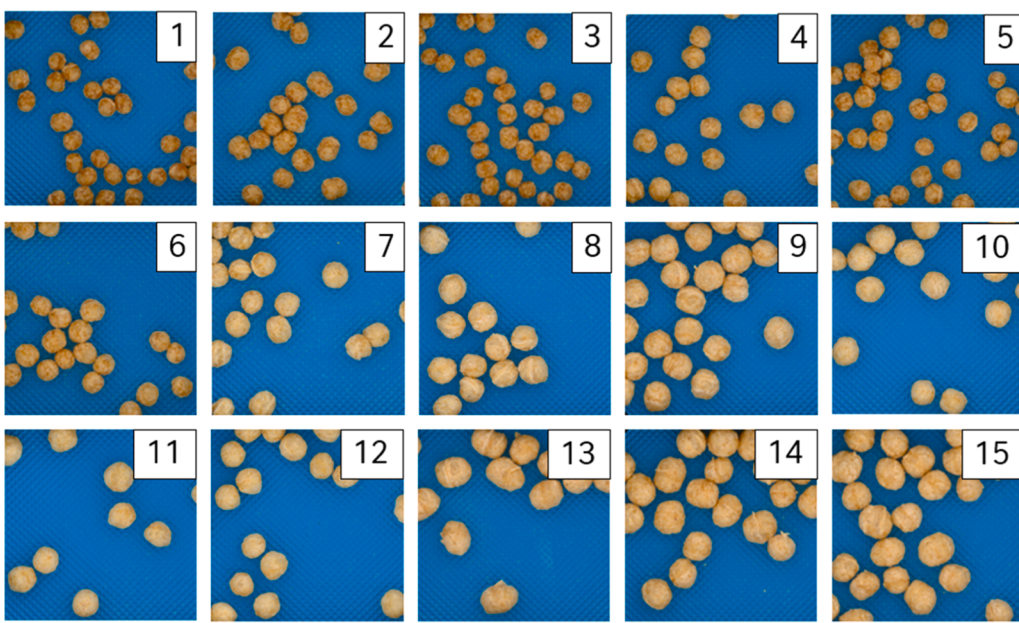


Fig. 5. Images of the 15 optimization samples captured by VideometerLab during trial #2.

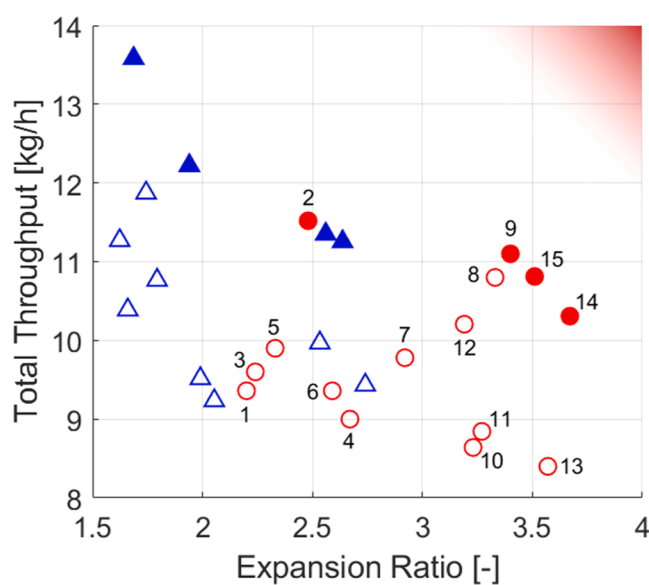


Fig. 6. Results and pareto front (●, ▲) between the expansion ratio and total throughput from trial #1 (Δ) and #2 (○). The optimal region of the design space defined by the objectives is indicated by the red shaded area.

this plot are more widely distributed, with no clustering around a specific region.

Throughput is primarily influenced by feed rate and screw speed (Morales Alvarez, 2020). As more material is fed into the extruder, a higher feed rate directly leads to an increased output, making it the main driver of throughput. In addition, increasing the screw speed improves the axial transport in the barrel, which shortens the residence time and contributes to a higher overall throughput. The data in Table 2 indicate that only the feed rate has a direct significant influence in this study. Besides four samples from the optimization (O2, O9, O14 and O15), another four sample points from the initial data set form the Pareto-front, reflecting the conditions that balance product structure with process efficiency, i.e. high product yield. One of the initial data points shows the highest throughput with 13.58 kg/h with a maximum

feed rate of 14.4 kg/h.

The sample points O9, O14, O15 from trial #2 and sample Δ2 from trial #1 stand out as high-performing solutions within the optimization space. Point O14 is Pareto-optimal across all three objectives - bulk density, throughput, and compactness - indicating a well-balanced extrusion condition that delivers highly expanded, uniformly shaped extrudates at efficient throughput. Points O9, O15 and Δ2 are optional candidates for suitable extrusion settings, especially in terms of expansion and shape, while still maintaining an efficient throughput. The high performing solutions were obtained under the assumption that all four objectives are equally important. The Pareto front therefore offers several suitable process settings that can be selected after the optimization depending on specific application needs or downstream goals.

When comparing the target temperatures and measured temperatures of the initial data set given in Table 2, most samples showed only minor deviations up to 5 °C. However, in four cases, the measured temperature exceeded the target - three times in barrel zone 2 and once in zone 4. This behavior was even more pronounced in the temperature profiles during the optimization. Fig. 7 (lower panel) visualizes the deviation of target temperature and measured temperature for the five zones and the 15 optimization experiments. A total of 10 out of 15 samples exhibited elevated values in barrel zone 4, while four samples showed increased temperatures in barrel zone 2. In each of these cases, the measured temperature was higher than the target due to thermal interference from a neighboring high-temperature zone.

As shown in Fig. 7 (upper panel), most temperature profiles suggested by TSEMO during the optimization experiments exhibited a typical "hump" shape (Schöppner and Resonnek, 2019), where the temperature peaked in the compression zone (zone 3) and was intended to decrease in the following metering section (zone 4). Such a profile is commonly employed to stabilize the melt viscosity before die exit, thus promoting optimal product expansion. In theory, reducing the temperature in zone 4 could help control rheological properties, minimize material degradation, and improve expansion behavior at the die.

However, the physical constraints of the extrusion process led to significant limitations. Zone 4 is thermally coupled with the neighboring high temperature zones, resulting in a situation where effective cooling of zone 4 was not feasible. Despite attempts to set lower temperatures, the actual measured values in zone 4 remained therefore elevated due to thermal conduction effects and the temperature profiles suggested by the optimization algorithm could not be realized in practice. Therefore,

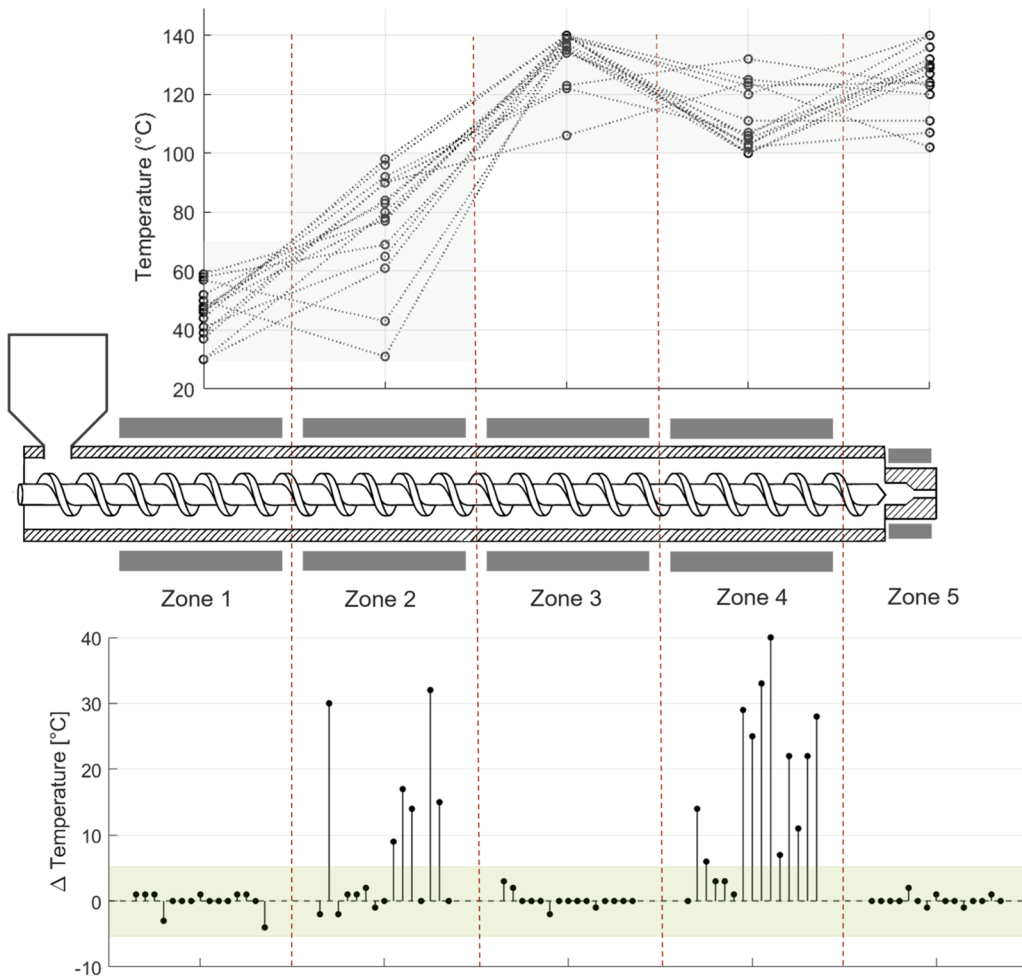


Fig. 7. Temperature profiles of the 15 optimization iterations as suggested by the TSEMO algorithm along the five barrel zones of the extruder (upper panel). The gray areas indicate the upper and lower temperature bound of each zone. The temperature values are illustrated by points and the dotted lines represent the connection between them. The deviation between target and measured temperature value for each zone during the 15 iterations (lower panel). The green area indicates the acceptable deviation of $\pm 5^{\circ}\text{C}$.

the algorithm TSEMO, operating on an exploration-exploitation basis, was fed with the measured temperatures, i.e. not its suggested ones. As a consequence, the model continuously identified this area of low temperature in zone 4 as underexplored and the optimizer repeatedly suggested similar settings near this infeasible region, attempting to gather more information and thereby introducing inefficiencies into the optimization process. Different approaches can be used to reduce or prevent this inefficiency. An easy to implement solution could be a feasibility screening of the candidates proposed and evaluated by NSGA-II prior to the hypervolume computation. Those candidates that exceed defined temperature differences between the zones would be excluded and thus not proposed for the next experimental extrusion round. While this method prevents technically unfeasible extrusion settings from being tested experimentally, no guidance of the optimizer or reduction of computational effort takes place. Another possibility is the integration of constraints, where a distinction is made between soft and hard constraints. A soft constraint can be realized by adding a fifth objective that models feasibility with a defined penalty function. Depending on the temperature difference between the barrel zones, this function will result in low values for feasible temperature settings and higher values for high temperature deviations between the zones. During the optimization process TSEMO tries to minimize this fifth objective function and learns therefore to avoid solutions with high penalty. While this method is not rejecting unfeasible settings, guidance of the optimization is guaranteed by informing the GP surrogate model. In the case of hard

constraint an inequality constraint function is integrated into the evaluation step of NSGA-II, impacting the ranking of possible candidates. Hereby, NSGA-II evolves over iterations towards feasible regions. For all three methods the acceptable temperature difference between the barrel zones must be defined based on the technical feasibility of the used extrusion set-up.

4. Conclusion

As the experimental results demonstrate, variations in screw speed, cutter speed, feed rate, moisture content and barrel temperature were found to have an impact on the expansion, shape, bulk density of direct-expanded products as well as the process efficiency. The manual optimization of four product characteristics by variation of nine process parameters is extremely challenging and has its limits due to the highly complex interdependence of process and product parameters. Using a BO algorithm coupled with the multi-objective optimizer NSGA-II and the hypervolume indicator as performance metric, a simultaneous progress towards multiple desired product characteristics could be achieved. By learning from an initial data set and iterative exploration and exploitation of the multidimensional design space, a product could be created that exhibits the desired properties and provides a successful trade-off between the objectives. In addition, the extrudates could be characterized on-line and in near real time due to the implementation of an automated analytical system. The combination of extrusion process,

automation and BO-supported optimization thus represents a time- and resource-saving method, and the results show the great potential of such a closed-loop framework to efficiently control low moisture extrusion processes. The current framework of this research focuses on process to product mapping, with equal importance of each objective and not direct link to end-user values, such as shelf-life or consumer satisfaction. With regard to the concept of closed-loop optimization investigated here, these end-user values are more difficult to capture through real-time measurements and without human input. Further models are needed that link measurable variables, such as those used within this work, with indicators of shelf life or sensory attributes.

CRediT authorship contribution statement

Deborah Becker: Writing – original draft, Visualization, Software, Methodology, Investigation, Formal analysis, Conceptualization. **Jean-Vincent Le Bé:** Writing – review & editing, Validation, Formal analysis. **Cornelia Rauh:** Supervision, Conceptualization. **Christoph Hartmann:** Writing – review & editing, Supervision, Funding acquisition, Conceptualization.

Declaration of competing interest

The authors declare that they have no known competing financial interests or personal relationships that could have appeared to influence the work reported in this paper.

Acknowledgements

Special appreciation goes to the Pilot Plant team and the Equipment Prototyping team for their great support (both located in Nestlé Research Lausanne - Strategic Research Operations).

Data availability

Data will be made available on request.

References

- Becker, D., Schmitt, C., Bovetto, L., Rauh, C., McHardy, C., Hartmann, C., 2023. Optimization of complex food formulations using robotics and active learning. *Innov. Food Sci. Emerg. Technol.* 83, 10323. <https://doi.org/10.1016/j.ifset.2022.103232>.
- Bouvier, J.-M., Campanella, O.H., 2014. The Generic Extrusion Process III. Eds.. In: Bouvier, J.-M., Campanella, O.H. (Eds.), *Extrusion Processing Technology: Food and Non-Food Biomaterials*. John Wiley & Sons Ltd., pp. 243–309. <https://doi.org/10.1002/9781118541685.ch6>
- Bradford, E., Schweidtmann, A.M., Lapkin, A., 2018. Efficient multiobjective optimization employing gaussian processes, spectral sampling and a genetic algorithm. *J. Glob. Optim.* 71, 407–438. <https://doi.org/10.1007/s10898-018-0609-2>.
- Carstensen, J.M., Frolm-Hansen, J., 2000. An apparatus and a method of recording an image of an object. European Patent EP1051660.
- Carstensen, J.M., 2018. LED spectral imaging with food and agricultural applications. In: Proc. SPIE 10656, *Image Sensing Technologies: Materials, Devices, Systems, and Applications V*, 1065604. <https://doi.org/10.1117/12.2304698>.
- Chinnaswamy, R., Hanna, M.A., 1988. Optimum extrusion-cooking conditions for maximum expansion of corn starch. *J. Food Sci.* 53 (3), 834–836. <https://doi.org/10.1111/j.1365-2621.1988.tb08965.x>.
- Deb, K., Pratap, A., Agarwal, S., Meyarivan, T., 2002. A fast and elitist multiobjective genetic algorithm: NSGA-II. *IEEE Trans. Evol. Comput.* 6, 182–197. <https://doi.org/10.1109/4235.996017>.
- Ditudompo, S., Takhar, P.S., Ganjyal, G.M., Hanna, M.A., 2016. Effect of extrusion conditions on expansion behavior and selected physical characteristics of cornstarch extrudates. *Trans. ASABE* 59 (4), 969–983. <https://doi.org/10.13031/trans.59.11467>.
- Egal, A., Oldewage-Theron, W., 2019. Extruded food products and their potential impact on food and nutrition security. *S. Afr. J. Clin. Nutr.* 33 (4), 142–143. <https://doi.org/10.1080/16070658.2019.1583043>.
- Ek, P., Ganjyal, G.M., 2020. Chapter 1 - basics of extrusion processing. Ed.. In: Ganjyal, G.M. (Ed.), *Extrusion Cooking*. Woodhead Publishing, pp. 1–28. <https://doi.org/10.1016/B978-0-12-815360-4.00016-X>.
- Fan, F.H., Ma, Q., Ge, J., Peng, Q.Y., Riley, W.W., Tang, S.Z., 2013. Prediction of texture characteristics from extrusion food surface images using a computer vision system and artificial neural networks. *J. Food Eng.* 118 (4), 426–433. <https://doi.org/10.1016/j.jfoodeng.2013.04.015>.
- Fulkerson, O., Inman, E., Rane, A., Noori, H., Deep, A., Ramesh, S., 2024. Multi-objective Bayesian optimization of fused filament fabrication parameters for enhanced specific fracture energy in PLA-carbon fiber composites. *Adv. Manuf.: Polym. Compos. Sci.* 10 (1). <https://doi.org/10.1080/20550340.2024.2395089>.
- Gomes, K.S., Berwian, G.F., Battistella, V.M.C., Bender, E.L., Reinehr, C.O., Colla, L.M., 2023. Nutritional and technological aspects of the production of proteic extruded snacks added of novel raw materials. *Food Bioprocess Technol.* 16, 247–267. <https://doi.org/10.1007/s11947-022-02887-0>.
- Kaur, N., Singh, B., Sharma, S., Kumar, R., 2022. Study of relationships between independent extrusion variables and dependent product properties during Quality Protein Maize extrusion. *Appl. Food Res.* 2 (1), 100048. <https://doi.org/10.1016/j.afres.2022.100048>.
- Kožić, J.S., Ilić, N.M., Kožić, P.S., Pezo, L.L., Banjac, V.V., Kruljić, J.A., Solarov, M.I.B., 2019. Multiobjective process optimization for betaine enriched spelt flour based extrudates. *J. Food Process. Eng.* 42, 12942. <https://doi.org/10.1111/jfpe.12942>.
- Kowalski, R.J., Li, C., Ganjyal, G.M., 2018. Optimizing twin-screw food extrusion processing through regression modeling and genetic algorithms. *J. Food Eng.* 234, 50–56. <https://doi.org/10.1016/j.jfoodeng.2018.04.004>.
- Kowalski, R.J., Piętrysiać, E., Ganjyal, G.M., 2021. Optimizing screw profiles for twin-screw food extrusion processing through genetic algorithms and neural networks. *J. Food Eng.* 303, 110589. <https://doi.org/10.1016/j.jfoodeng.2021.110589>.
- Kristiawan, M., Guessasma, S., Della Valle, G., 2020. Chapter 10 - extrusion cooking modeling, control, and optimization. Ed.. In: Ganjyal, G.M. (Ed.), *Extrusion Cooking*. Woodhead Publishing, pp. 295–330. <https://doi.org/10.1016/B978-0-12-815360-4.00010-9>.
- Lai, L.S., Kokini, J.L., 1991. Physicochemical changes and rheological properties of starch during extrusion (a review). *Biotechnol. Prog.* 7 (3), 251–266. <https://doi.org/10.1021/bp00009a009>.
- Mezreb, K., Goullieux, A., Ralainirina, R., Queneudec, M., 2003. Application of image analysis to measure screw speed influence on physical properties of corn and wheat extrudates. *J. Food Eng.* 57 (2), 145–152. [https://doi.org/10.1016/S0260-8774\(02\)00292-3](https://doi.org/10.1016/S0260-8774(02)00292-3).
- Mitra, P., Ramaswamy, H., 2021. Artificial Neural Network (ANN) modeling to predict the twin-screw extrusion processing variables of soy protein isolate and corn flour blend formulations on the physical properties of extrudates. *J. Saudi Soc. Food Nutr.* 14 (1), 55–67. <https://search.emarefa.net/detail/BIM-1334750>.
- Morales Alvarez, J.C., 2020. Chapter 2 - engineering aspects of extrusion: extrusion processing as a multiple-input and multiple-output system. Ed.. In: Ganjyal, G.M. (Ed.), *Extrusion Cooking*. Woodhead Publishing, pp. 29–71. <https://doi.org/10.1016/B978-0-12-815360-4.00002-X>.
- Morantes, G., Ek, P., Ganjyal, G.M., 2020. Chapter 16 - food safety in extrusion processing. Ed.. In: Ganjyal, G.M. (Ed.), *Extrusion Cooking*. Woodhead Publishing, pp. 507–521. <https://doi.org/10.1016/B978-0-12-815360-4.00016-X>.
- Myung, J.I., Deneault, J.R., Chang, J., Kang, I., Maruyama, B., Pitt, M.A., 2025. Multi-objective bayesian optimization: a case study in material extrusion. *Digit. Discov.* 4, 723. <https://doi.org/10.1039/D4DD00320A>.
- Patil, S., Kaur, C., 2018. Current trends in extrusion: development of functional foods and novel ingredients. *Food Sci. Technol. Res.* 24 (1), 23–34. <https://doi.org/10.3136/FSTR.24.23>.
- Riaz, M.N., 2019. Chapter 19- food extruders. Ed.. In: Kutz, M. (Ed.), *Handbook of Farm, Dairy and Food Machinery Engineering*, 3rd Edition. Elsevier, pp. 483–497. <https://doi.org/10.1016/B978-0-12-814803-7.00019-1>.
- Sahu, C., Patel, S., Tripathi, A.K., 2022. Effect of extrusion parameters on physical and functional quality of soy protein enriched maize based extruded snack. *Appl. Food Res.* 2 (1), 100072. <https://doi.org/10.1016/j.afres.2022.100072>.
- Schöppner, V., Resonnek, V., 2019. Investigation of the barrel temperature profile on the process behavior of single screw extruders and strategies to determine the optimal temperature control. *AIP. Conf. Proc.* 2139 (1), 020003. <https://doi.org/10.1063/1.5121650>.
- Schulz, E., Speekenbrink, M., Krause, A., 2018. A tutorial on Gaussian process regression: modelling, exploring, and exploiting functions. *J. Math. Psychol.* 85, 1–16. <https://doi.org/10.1016/j.jmp.2018.03.001>.
- Shah, F.-u-H., Sharif, M.K., Ahmad, Z., Amjad, A., Javed, M.S., Suleman, R., Sattar, D.-e-S., Amir, M., Anwar, M.J., 2022. Nutritional characterization of the extrusion-processed micronutrient-fortified corn snacks enriched with protein and dietary fiber. *Front. Nutr.* 9, 1062616. <https://doi.org/10.3389/fnut.2022.1062616>.
- Tachibana, R., Zhang, K., Zou, Z., Burgenet, S., Ward, T.R., 2023. A customized bayesian algorithm to optimize enzyme-catalyzed reactions. *ACS Sustain. Chem. Eng.* 11 (33), 12336–12344. <https://doi.org/10.1021/acssuschemeng.3c02402>.
- Theng, A.H.P., Lakshminarayanan, M., Ong, D.S.M., Hua, X.Y., Foo, C.S., Khoo, E., Chiang, J.H., 2025. Multi-objective Bayesian optimisation on the textual properties of plant-based meat analogues through high-moisture extrusion. *J. Food Eng.* 396, 112566. <https://doi.org/10.1016/j.jfoodeng.2025.112566>.